JOURNAL OF APPLIED ELECTROCHEMISTRY 13 (1983) 365–370

Galvanic cell-type humidity sensor using high temperature-type proton conductive solid electrolyte

H. IWAHARA, H. UCHIDA, J. KONDO

Department of Environmental Chemistry and Technology, Faculty of Engineering, Tottori University, Koyamacho, Tottori 680, Japan

Received 21 July 1982

Galvanic cell, humidity sensors were investigated using a high temperature proton conductive solid electrolyte based on $SrCeO_3$. A sensor of this type is one of the applications of a steam concentration cell, the concept of which was recently discussed. These sensors could be operated stably at elevated temperatures. Furthermore, they exhibit a linear e.m.f. response against logarithm of vapour pressure over a wide range, a good reproductibility, a very fast response time and small responses to impurity gases.

1. Introduction

Recently we found that some sintered oxides based on $SrCeO_3$ exhibited proton conduction under hydrogen- or water-containing atmospheres at high temperatures [1–3]. As a result, a concept of steam concentration cell was proposed and, verified experimentally [1, 4]. One possible application of the steam concentration cell will be a galvanic cell-type humidity sensor which had not previously been reported.

In contrast to the conventional humidity sensors, which are based on the change in conductance or capacitance of a solid on adsorbing water vapour [5–10], the galvanic sensor proposed here may, in principle, have the following features; (a) the humidity is given directly by the e.m.f. of galvanic cell, (b) the working temperature can be high because protonic conduction in the ceramics appears at elevated temperatures, the working temperature of the conventional sensor is below 160° C [10].

In this study, the galvanic humidity sensors were constructed using high temperature, proton conductors based on $SrCeO_3$ and their performances were examined. These sensors exhibited a stable operation over a wide humidity range, a very fast response time and relatively small responses to impurity gases.

2. Working principles of the sensor

As illustrated in Fig. 1, a gas cell constructed with a proton conductive ceramic as the electrolyte gives rise to an e.m.f. due to the concentration difference of water vapour, when atmospheres with different humidities are introduced into each electrode compartment [1, 4].

The theoretical e.m.f., E_0, can be written as

$$E_0 = \frac{RT}{2F} \ln \frac{P_{H_2O}(I)}{P_{H_2O}(II)} \left(\frac{P_{O_2}(II)}{P_{O_2}(I)} \right)^{1/2} \quad (1)$$

where P_{H_2O} and P_{O_2} are the partial pressure of water vapour and oxygen, respectively, and R, F and T have their usual meanings.

When $P_{O_2}(I)$ is close to $P_{O_2}(II)$, as in ambient atmospherics with different humidities, E_0 can be written as

$$E_0 = \frac{RT}{2F} \ln \frac{P_{H_2O}(I)}{P_{H_2O}(II)} \quad (2)$$

If $P_{H_2O}(II)$ is known and is constant, the humidity in the compartment I (or $P_{H_2O}(I)$) may be estimated from the measured e.m.f. of the cell.

When an electrolyte involves electronic conduction, e.m.f. is lowered to some extent

$$E \leqq t_{H^+} \cdot E_0 \quad (3)$$

where t_{H^+} is the transference number of the

0021-891X/83 $03.00 + .12.

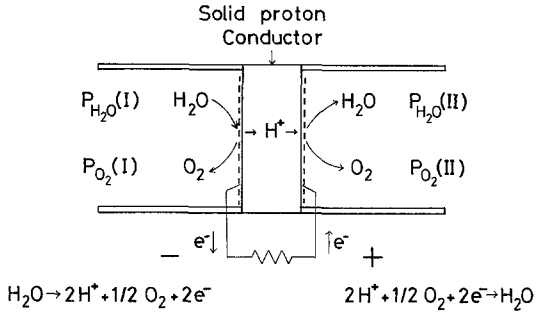

Fig. 1. The concept of a steam concentration cell using solid proton conductor. $P_{H_2O}(I) > P_{H_2O}(II)$.

proton in the solid electrolyte. Even in such a case, we can determine $P_{H_2O}(I)$ from the measured e.m.f. by using a calibration curve.

3. Experimental details

The proton conducting ceramics used in this study were $SrCe_{0.95}Yb_{0.05}O_{3-\alpha}$ (α is the number of deficiencies per perovskite unit cell). The preparations of the ceramics were the same as in the previous study [1]. The dense sinters obtained were sliced into thin discs (thickness: about 0.5 mm, diameter 12 mm) to provide the electrolyte diaphragms for the gas cells.

The construction of the galvanic humidity sensor is illustrated in Fig. 2. Each face of solid

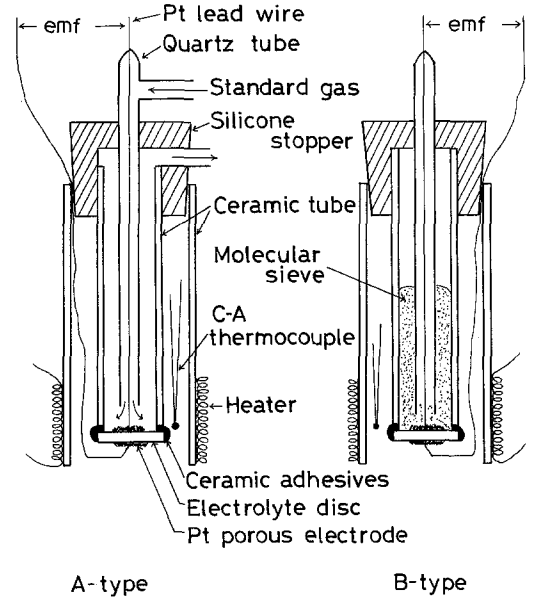

Fig. 2. Schematic illustrations of the galvanic cell-type humidity sensors.

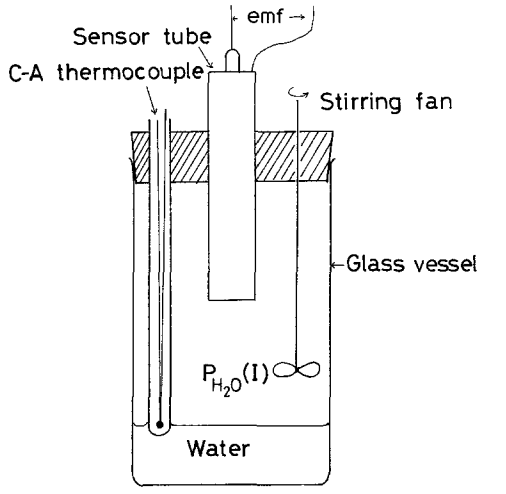

Fig. 3. Setting of the sensor tube in the test chamber.

electrolyte diaphragm was smeared with platinum paste and baked at 1000° C to provide a porous electrode material. The specimen electrolyte thus obtained was attached to a ceramic tube by ceramic adhesives based on Al_2O_3 (Sumiceram®). Thus, two electrode compartments, inside and outside of the tube, were separated by the specimen electrolyte. The electrolyte was heated by a nichrome wire heater wound around the outer tube of the sensor.

As is clear from Equation 4, it is necessary to keep either $P_{H_2O}(I)$ or $P_{H_2O}(II)$ constant in order to obtain a steady e.m.f. response to a given humidity. Two types of sensors were examined. One is a gas flow type (A-type in Fig. 2) in which air saturated with water vapour at 0° C was passed through the inner electrode compartment (inside of the tube - $P_{H_2O}(II) = 4.6$ torr). Another is a packed construction (B-type in Fig. 2) in which a molecular sieve is used to keep the vapour pressure inside the tube constant. As shown in Fig. 3 the sensor tube was set in a glass vessel (volume: about 1000 cm^3) settled in a thermostat. A small stirring fan was placed in the vessel.

The humidity in the vessel (outside of the tube) was controlled by regulating the temperature of water at the bottom of the vessel. The temperature of water was controlled within ± 1° C accuracy. In this study, the humidity in the vessel was represented by the partial pressure of water (torr), assuming that the gas in the vessel (normally, air) was completely saturated with water.

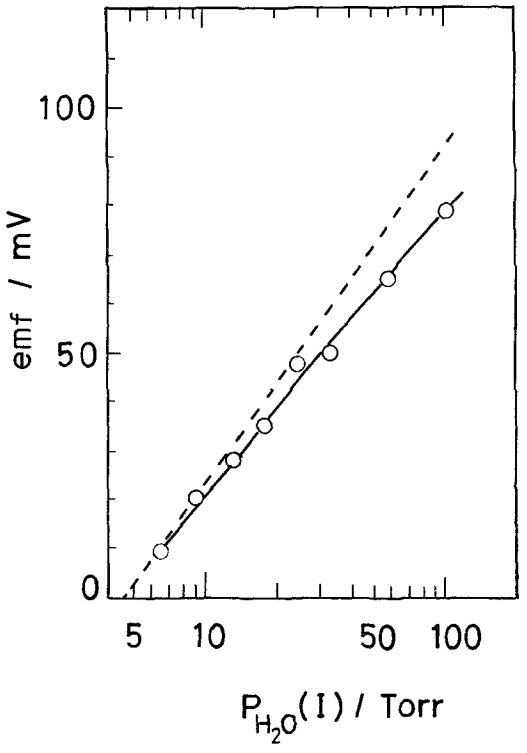

Fig. 4. E.M.F. response of the A-type sensor to P_{H_2O}(I). Working temperature; 400° C (broken line shows theoretical E.M.F. calculated from Equation 2).

The e.m.f. of the sensor was measured by a conventional electrometer. Also, the e.m.f. and the temperature of water were recorded simultaneously by a recorder.

Prior to the initial measurement, the sensor was heated overnight to 400° C in order to eliminate the impurities from the ceramic adhesives.

4. Results and discussion

4.1. *E.M.F. response to the humidity*

Fig. 4 shows the e.m.f. response of the A-type sensor to the logarithm of P_{H_2O}(I) at 400° C using $SrCe_{0.95}Yb_{0.05}O_{3-\alpha}$ as the electrolyte. The sensor exhibited a stable, good, linear response against the logarithm of P_{H_2O} and good agreement with the theoretical e.m.f. value calculated from Equation 2. There was no change in the e.m.f. on stirring with the fan in the vessel, but the response time became somewhat faster.

The response of the e.m.f. following an increase or decrease in humidities were examined by changing the temperature of the vessel gradually. Fig. 5 shows the results. The e.m.f. against time curve is almost parallel to the temperature against time curve during increasing humidity, and, during the humidity decrease, the change in e.m.f. with time corresponds to the change in temperature with time.

To examine the rapid response characteristics, the humidity in the vessel was changed quickly by injecting hot water into the bottom of the vessel. The e.m.f. of the sensor increased rapidly corresponding to the rise of the temperature of the water as shown in Fig. 6. It took only a few seconds for the e.m.f. to establish a stable value after the vapour pressure was changed rapidly from 12 to 20 torr.

4.2. *Some improvement of the sensor*

It may be unfavourable for a practical sensor to use a flow of standard humidity gas. So, we

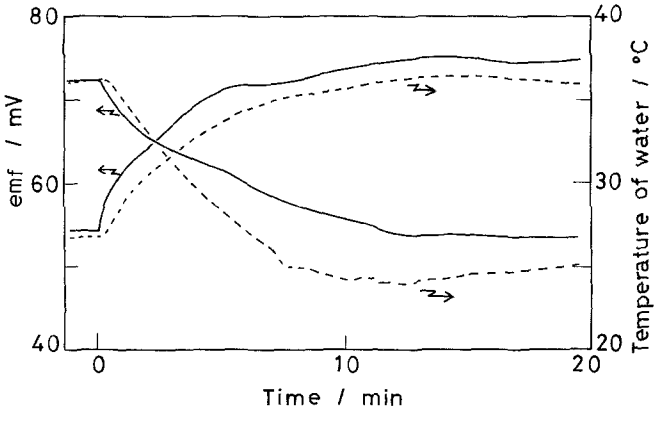

Fig. 5. Change in e.m.f. response during increase or decrease in the P_{H_2O}(I). A-type sensor (working temperature; 400° C) —— e.m.f. response, – – – temperature of water.

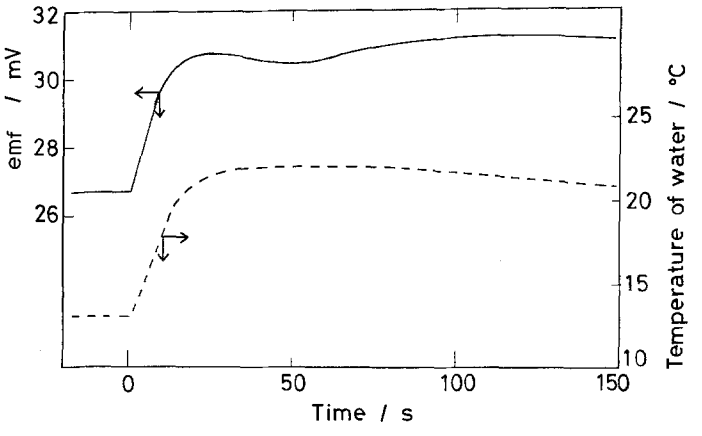

Fig. 6. E.M.F. response of the A-type sensor on rapid increase in the P_{H_2O}(I) (working temperature; 400° C).

examined the B-type sensor described in Section 3.

Fig. 7 shows the e.m.f. response of this type of sensor at 300 ~ 400° C. This sensor exhibited a good linear response of e.m.f. against the logarithm of P_{H_2O}. The e.m.f. at 400° C was expressed as

$$E(\text{mV}) = -23.0 + 93.7 \log P_{H_2O} \text{ (torr)}$$

with a standard deviation of 4.6 mV for $P_{H_2O} = 10 \sim 100$ torr. Due to the lower vapour pressure inside the tube compared to the case of the A-type sensor, the e.m.f. of the B-type sensor is higher than that of the A-type one. Since the equilibrium vapour pressure inside the tube becomes lower with decreasing temperatures, it is reasonable that the e.m.f.'s at lower temperatures are larger than those at higher temperatures. Similarly to the A-type sensor, the response of the B-type sensor was also rapid (within a few seconds).

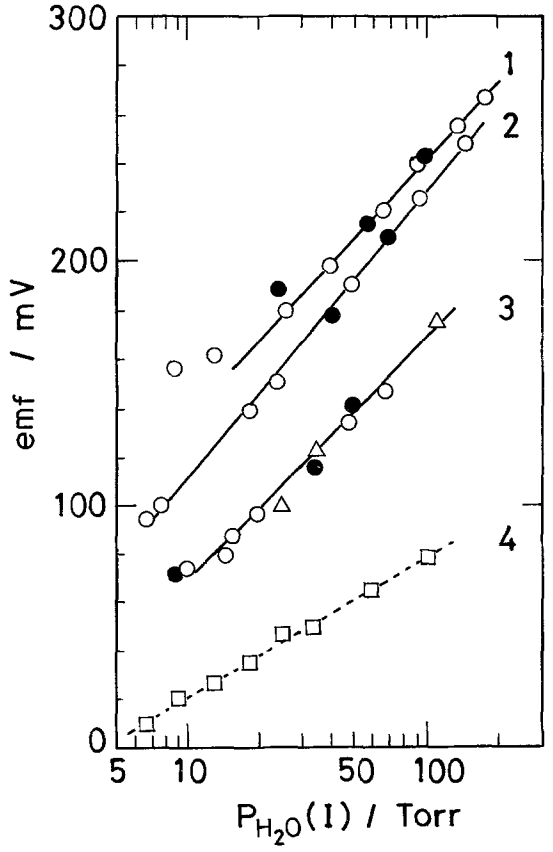

Fig. 7. E.M.F. response of the B-type sensor (lines 1 to 3) and the A-type sensor (line 4) to P_{H_2O}(I). Working temperature: 1;300° C, 2;350° C, 3 and 4;400° C. ○ 1st increasing the P_{H_2O}(I), ● 1st decreasing, △ 2nd increasing.

The sensitivity of the sensor was determined from Fig. 7 and listed in Table 1. The B-type sensor had a higher sensitivity than the A-type. However, the sensitivity of the B-type exceeded the theoretical value (= 2.30 $RT/2F$).

This phenomenon can be explained by considering the proton transference number, t_{H^+}, in $SrCe_{0.95}Yb_{0.05}O_{3-\alpha}$ electrolyte. As described previously [1, 4], conduction in these ceramics is not purely ionic but partially electronic, and

Table 1. Sensitivity of the galvanic cell-type sensor at 400° C

	Sensitivity (mV decade^{-1})
A-type	58.0
B-type	93.7
Theoretical (2.303 $RT/2F$)	66.7

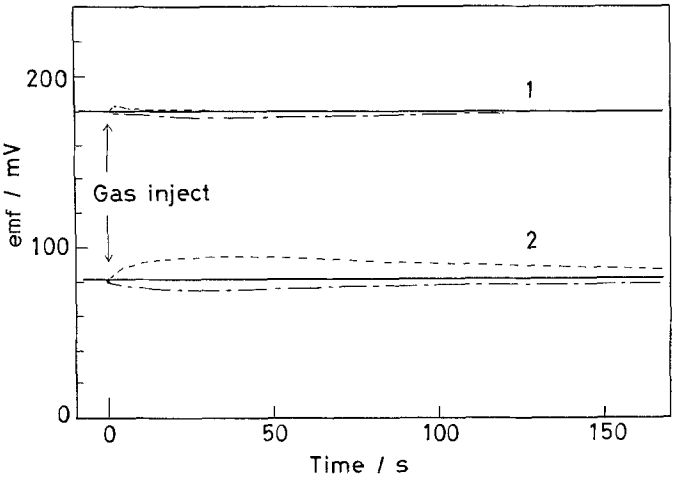

Fig. 8. Response of the B-type sensor to the impurity gas injection impurity gas; ———— H_2, –·– C_4H_{10}, —— none and CO_2. Working temperature: 1, 300° C; 2, 400° C.

the transference number of proton at very low vapour pressure is small. In the case of the A-type sensor, the vapour pressure at the standard electrode inside the tube is not so low (4.6 torr) so that t_{H^+} of the electrolyte can be regarded as almost constant (about 0.9, from Fig. 4) irrespective of the vapour pressure outside of the tube (P_{H_2O}(I)).

On the other hand, in the case of the B-type sensor, the humidity inside the sensor tube has a much lower value than in the case of the A-type. Also t_{H^+} may decrease with decreasing vapour pressure in the outer atmosphere. As a result, the gradient of E against $\log P_{H_2O}$ (I) is steep. The detailed studies of the dependence of the t_{H^+} of the specimen electrolyte upon the P_{H_2O} are in progress.

4.3. *Response to the impurity gas*

The effects of some impurity gases on the e.m.f. response of the B-type sensor were tested as follows. Air (flow rate = 100 cm^3 min^{-1}) in the laboratory room (60% RH, 17° C, P_{H_2O} = 8.7 torr) was introduced to the glass vessel. When the sensor exhibited a constant e.m.f. response, 100 μl of impurity gas was injected into the vessel with the flow of air. Hydrogen, butane and carbon dioxide were injected as the impurity gas.

The e.m.f. response and the maximum deviation from the usual humidity response were shown in Fig. 8 and Table 2, respectively. Hydrogen gas made the e.m.f. increase. This is reasonable because the electrolyte of the sensor is a proton conductor. On the other hand, there was no change in the e.m.f. for the injection of carbon dioxide, even if a few cm^3 of carbon dioxide was injected. Butane gas made the e.m.f. decrease somewhat, probably because of its adsorption to the electrode surface instead of water vapour. However, the e.m.f. change caused by the impurity gas injection was relatively small compared with the e.m.f. response to the humidity, especially at 300° C (Table 2).

According to Equation 1, this sensor responds to any pressure difference in oxygen between two electrode compartments. However, we can determine the vapour pressure by using a calibration curve if the pressure difference in oxygen is constant. Furthermore, even if oxygen pressures at both electrodes are variable, we can cancel the e.m.f. due to oxygen pressures by connecting galvanic cell-type oxygen sensor electrically to this sensor in series.

Table 2. Deviation of the e.m.f. from the usual humidity response caused by the impurity gas injection

Impurity gas	*Maximum deviation of the e.m.f.* (%)	
	300° C	400° C
H_2	+ 0.78	+ 17.0
C_4H_{10}	− 1.7	− 6.3
CO_2	± 0.0	± 0.0

Acknowledgement

This work was partially supported by Grant-in-Aid for Special Research 'New Investigation of

Functional Ceramics' funded by the Ministry of Education, Science and Culture, Japan.

References

[1] H. Iwahara, T. Esaka, H. Uchida and N. Maeda, *J. Solid State Ionics* **3/4** (1981) 359.
[2] H. Iwahara, H. Uchida and T. Esaka, *Prog. Batteries Solar Cells* **4** (1982) 279.
[3] H. Iwahara, H. Uchida and N. Maeda, *J. Power Sources* **7** (1982) 293.
[4] H. Uchida, N. Maeda and H. Iwahara, *J. Appl. Electrochem.* **12** (1982) 645.
[5] H. Arai, *Denki Kagaku* **50** (1982) 38.
[6] K. Kanoh and K. Kawasaki, *Jpn. J. Electron.* **1966** (1966) 2172.
[7] T. Kawasaki, Z. Minowa and T. Inamatsu, *Oyo Butsuri* **35** (1966) 355.
[8] N. Ichinose, Y. Yokomizo and M. Katura, *Denshi Zairyo* **1977** (1977) 69.
[9] T. Nitta, Z. Terada and S. Hayakawa, *J. Amer. Ceram. Soc.* **63** (1980) 295.
[10] I. G. Young, *ISA Trans.* **11** (1972) 65.